

## Conformation and Monolayer Assembly Structure of a Pentiptycene-Derived $\alpha,\omega$ -Alkanedithiol†

Jye-Shane Yang,<sup>\*,‡</sup> Chung-Chieh Lee,<sup>‡</sup> Shuen-Lin Yau,<sup>‡</sup> Chin-Chi Chang,<sup>‡</sup>  
Cheng-Chung Lee,<sup>§</sup> and Jian-Ming Leu<sup>§</sup>

Department of Chemistry and Institute of Optical Sciences, National Central University,  
Chung-Li, Taiwan 32054

Received August 24, 1999

The synthesis, conformation, and monolayer assembly structure of a pentiptycene-derived  $\alpha,\omega$ -alkanedithiol (**1**) are reported. The results of MM2 modeling, the scanning tunneling microscopy (STM), and the surface plasmon resonance (SPR) suggest that **1** favors a folded conformation, corresponding to a looped monolayer assembly structure, on the Pt(111) and Au(111) surfaces. Nonetheless, the conformation of **1** in the crystals might be an extended form according to the crystal structure of an analogous compound **4**. The relative interchain interactions and packing densities can account for the choice between a folded and an extended conformation for **1** in the condensed phases.

### Introduction

The self-assembly of organic compounds on metal surfaces provides a unique platform for the investigation of molecular structures and intermolecular interactions in a two-dimensional region. Mechanistic studies on the alkanedithiol/Au(111) systems have revealed a phase transition from a surface-aligned (lie-down) to a surface normal-aligned (stand-up) structure during the formation of self-assembled monolayers (SAMs).<sup>1</sup> While this is consistent with a close packing behavior of organic compounds in the crystals to maximize molecular nonbonded (e.g., van der Waals, electrostatic) interactions,<sup>2</sup> a decrease of SAM ordering for short chain alkanedithiols suggests that only sufficient interchain interactions can effectively induce the phase transition and crystalline order.<sup>3</sup> In addition, while the thiolate chemisorption is closely associated with the adsorbate lattice on the metal substrate (e.g., 5 and 4.4 Å of spacing on gold and on silver, respectively), the interchain interactions are responsible for the observed tilt angle of alkyl chains (e.g.  $\sim 30^\circ$  on gold and  $\sim 11^\circ$  on silver with respect to the surface normal).<sup>4</sup> Theoretical studies also support the importance of interchain interactions, as the calculated van der Waals energies for long alkanedithiols (>10 carbons) can be comparable to the S–Au chemisorption energy ( $\sim 28$  kcal/mol).<sup>4,5</sup> The understanding of two-dimensional monolayer nonbonded forces and adsorbate–substrate chemisorption behavior is thus the premise to the construction of monolayers having desired organizations and properties.

To this end, the conformation and monolayer structure of  $\alpha,\omega$ -dithiols on metal surfaces are of great interest in their uses to fabricate molecular devices.<sup>6,7</sup> The dithiol termini enable  $\alpha,\omega$ -dithiols to serve as molecular wires connecting to two metal substrates when a stand-up structure is adopted (Figure 1A).<sup>8</sup> However, both thiol termini can chemisorb on the same substrate leading to a lie-down (Figure 1B) or a looped structure (Figure 1C) depending on the extent of adsorbate–substrate contact. Although the lie-down structure is less favorable for monothiol compounds on the metal surface, it should be more competitive in the case of  $\alpha,\omega$ -dithiols because of the presence of an additional thiolate chemisorption. Nonetheless, the stand-up structure is still preferred for most rod-shaped  $\alpha,\omega$ -dithiols containing alkyl, conjugated, or the hybrid molecular backbones,<sup>6–8</sup> and the lie-down or the looped structure has been rare.<sup>9,10</sup> Moreover, the monolayer organization of  $\alpha,\omega$ -dithiols could be strongly surface dependent.<sup>9</sup> While these observations are not fully explained, they show the fine interplay between intermolecular nonbonded interactions and adsorbate–substrate interactions. Other driving forces are required to allow  $\alpha,\omega$ -dithiols to adopt the lie-down or the looped structure instead of the prevailing stand-up organizations.

The novel three-dimensional structures of iptycenes, such as triptycene and pentiptycene, have demonstrated particular utility in the formation of sensors,<sup>11</sup> liquid

(6) Nakamura, T.; Kondoh, H.; Matsumoto, M.; Nozoye, H. *Langmuir* **1996**, *12*, 5977–5979.

(7) (a) Tour, J. M.; Jones, L., II.; Pearson, D. L.; Lamba, J. J. S.; Burgin, T. P.; Whitesides, G. M.; Allara, D. L.; Parikh, A. N.; Atre, S. V. *J. Am. Chem. Soc.* **1995**, *117*, 9529–9534. (b) Kohli, P.; Taylor, K. K.; Harris, J. J.; Blanchard, G. J. *J. Am. Chem. Soc.* **1998**, *120*, 11962–11968.

(8) (a) Brust, M.; Bethell, D.; Schiffrin, D. J.; Kiely, C. J. *Adv. Mater.* **1995**, *7*, 795–797. (b) Ardres, R. P.; Bielefeld, J. D.; Henderson, J. I.; Janes, D. B.; Kolagunta, V. R.; Kubiak, C. P.; Mahoney, W. J.; Osifchin, R. G. *Science* **1996**, *273*, 1690–1693. (c) Resch, R.; Baur, C.; Bugacov, A.; Koel, B. E.; Echternach, P. M.; Madhukar, A.; Montoya, N.; Requicha, A. A. G.; Will, P. *J. Phys. Chem.* **1999**, *103*, 3B, 3647–3650.

(9) Murty, K. V. G. K.; Venkataraman, M.; Pradeep, T. *Langmuir* **1998**, *14*, 5446–5456.

(10) Obeng, Y. S.; Laing, M. E.; Friedli, A. C.; Yang, H. C.; Wang, D.; Thulstrup, E. W.; Bard, A. J.; Michl, J. *J. Am. Chem. Soc.* **1992**, *113*, 9943–9952.

\* To whom correspondence should be addressed. E-mail: jsyang@rs250.ncu.edu.tw.

† Dedicated to Professor Kwang-Ting Liu on the occasion of his 60th birthday.

‡ Department of Chemistry.

§ Institute of Optical Sciences.

(1) Poirier, G. E.; Pylant, E. D. *Science* **1996**, *272*, 1145–1148.

(2) Desiraju, G. R. *Crystal Engineering-The Design of Organic Solids*; Elsevier: New York, 1989; Chapter 2.

(3) Porter, M. D.; Bright, T. B.; Allara, D. L.; Chidsey, C. E. D. *J. Am. Chem. Soc.* **1987**, *109*, 3559–3568.

(4) Sellers, H.; Ulman, A.; Shnidman, Y.; Eilers, J. E. *J. Am. Chem. Soc.* **1993**, *115*, 9389–9401.

(5) Nuzzo, R. G.; Zegarski, B. R.; Dubois, L. H. *J. Am. Chem. Soc.* **1987**, *109*, 733–740.

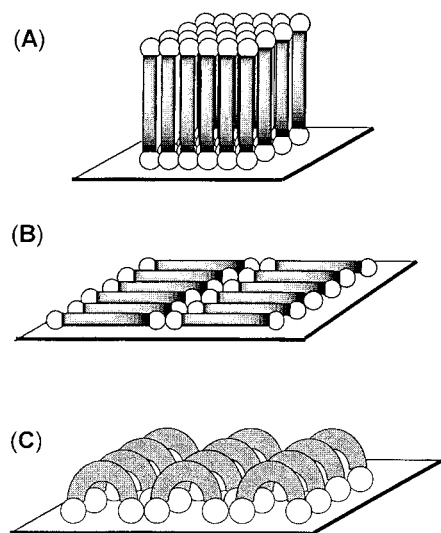


**Figure 1.** Schematic representations of three distinct orientations of  $\alpha,\omega$ -dithiols on the metal surface corresponding to the (A) stand-up, (B) lie-down, and (C) looped monolayer assembly structures.

crystals,<sup>12</sup> catalysts,<sup>13</sup> and molecular electronics.<sup>14</sup> We are thus interested in the construction of a SAM having the aromatic functionalities of iptycenes at the monolayer-air/liquid interface for potential applications. In this paper, we report the synthesis of an  $\alpha,\omega$ -alkanedithiol containing the pentiptycene groups (**1**) and its conformational characterization by crystallography, MM2 modeling, scanning tunneling microscopy (STM), and surface plasmon resonance (SPR). Our results indicate that a folded conformation of **1** is energetically more stable than an extended one in the gas phase; however, intermolecular interactions play an important role in the choice between the folded and the extended conformation for **1** in the condensed phases. While **1** adopts a folded conformation corresponding to a looped monolayer assembly structure on the metal surface, an extended conformation appears to be the case in the crystals.

## Results and Discussion

The pentiptycene-incorporated  $\alpha,\omega$ -alkanedithiol **1** was prepared from the precursor of pentiptycene hydroquinone **3**, which was in turn obtained from the reduction of pentiptycene quinone **2** using sodium hydrosulfite (Scheme 1). One of us has previously reported a simple procedure for a multigram synthesis of **2** from the commercially available anthracene and benzoquinone.<sup>11</sup> Alkylation of **3** with 10-undecenyl tosylate<sup>15</sup> afforded the compound **4**, which was then converted to the dithioesters **5** in a thermally activated radical addition of thioacetic acid to the terminal double bonds. Acid-catalyzed hydrolysis of **5** gave the desired product **1** in an excellent yield.

Compound **4** crystallizes in a needle form, and its single-crystal X-ray structure was determined.<sup>16</sup> Two

crystallographically independent conformers (**4a** and **4b**) that mainly differ in their terminal chain conformations are both in an extended conformation (Figure 2A). Despite some extent of disorder in the aliphatic terminals leading to relatively high discrepancy index values (*R* or *wR*), its unambiguous crystal packing can provide us a clue to the question as to how the pentiptycene groups arrange themselves in the space. As is schematically depicted in Figure 2B, the pentiptycene groups of each conformer **4a** and conformer **4b** construct two-dimensional porous layers parallel with the (001) lattice plane, which pack along the *c* direction of crystal lattice in an alternating manner. It has been previously demonstrated that iptycene derivatives in the solid state tend to form cavities, in which solvent molecules are usually included.<sup>11,17</sup> However, instead of the solvent inclusion, each cavity in the **4a** layer is threaded by two aliphatic chains from its two neighboring conformers **4b** (one above and the other below the layer) and vice versa. The interpenetrating packing of aliphatic chains is apparently to reduce the void space and, meanwhile, to increase the interchain interactions in the crystals. Although a single-crystal X-ray structure of **1** has not been obtained, it is expected to adopt crystal packing in a way similar to that of **4**. In general, the sulfur atom as well as the thiol group only participate in normal van der Waals contacts and play its part in the crystal structure according to its geometrical properties.<sup>18</sup>

Since the observed interlayer threading is a phenomenon of three-dimensional crystal packing, the resulting interlayer interactions will disappear in a two-dimensional monolayer structure. As a result, the conformation of **1** in the monolayer could be very different from that in the crystals. Two distinct molecular conformations and the corresponding SAM structures are considered here for  $\alpha,\omega$ -dithiol **1**. For an extended conformation of **1**, the layer structure of the analogous compound **4** in the crystals (Figure 2B) provides a reasonable model for a possible stand-up monolayer assembly. As is schematically shown in Figure 3A, the intermolecular sulfur-to-sulfur distances, which are mainly determined by the rigid and bulky pentiptycene groups, can be estimated on the basis of the crystallographic data of **4**. The corresponding packing density is  $\sim 165 \text{ \AA}^2$  per molecule. Other stand-up monolayer arrangements with greater packing densities are surely possible, but the pentiptycene dimensions seems less likely to allow **1** to have a packing density larger than  $110 \text{ \AA}^2/\text{molecule}$ . On the other hand, a SAM structure resulting from a folded **1** is schematically proposed in Figure 3B, in which several

(16) Data for the X-ray structure were recorded using a Siemens SMART/CCD diffractometer at  $-120 \text{ }^\circ\text{C}$ . The terminal chain disorder is even more significant when data was collected at room temperature, but the rest part of the molecule as well as the overall crystal packing are nearly not affected. Since the terminal regions of the aliphatic chains are located at the cavities created by pentiptycene groups, this indicates that the size of cavities is larger than that of their occupants, the aliphatic chains. In addition, the inevitable terminal chain disorder instead of the quality of the crystal should be responsible for the high discrepancy index values. The following are data for the crystal system, space group, unit cell parameters ( $\text{\AA}$  and degree), *Z*, *R*, *wR*, and GOF: triclinic, *P*1, *a* = 12.2691(2), *b* = 13.6644(2), *c* = 15.8290(2),  $\alpha$  = 65.349(1),  $\beta$  = 67.588(1),  $\gamma$  = 82.818(1), 2, 0.0974, 0.2650, 1.079.

(17) (a) Wilcox, C. F.; Roberts, F. D. *J. Org. Chem.* **1965**, *30*, 1959–1963. (b) Bashir-Hashemi, A.; Hart, H.; Ward, D. L. *J. Am. Chem. Soc.* **1986**, *108*, 6675–6679. (c) Venugopalan, P.; Bürgi, H.-B.; Frank, N. L.; Baldrige, K. K.; Siegel, J. S. *Tetrahedron Lett.* **1995**, *36*, 2419–2422.

(18) Desiraju, G. R. *Crystal Engineering-The Design of Organic Solids*; Elsevier: New York, 1989; Chapter 7.

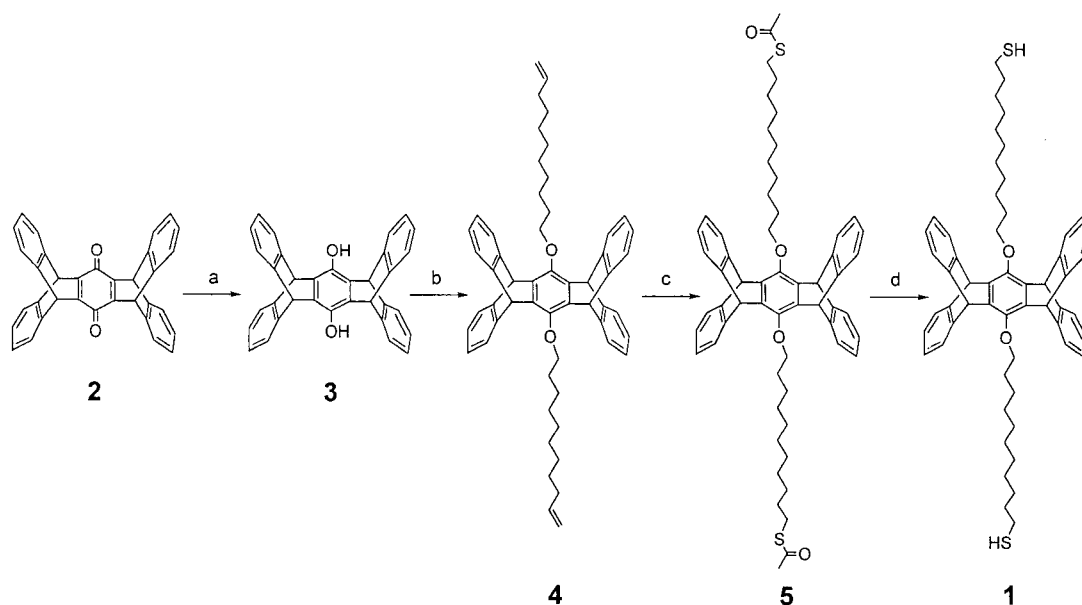
(11) Yang, J.-S.; Swager, T. M. *J. Am. Chem. Soc.* **1998**, *120*, 11864–11873.

(12) Norvez, S. *J. Org. Chem.* **1993**, *58*, 2414–2418.

(13) Ramondenc, Y.; Schwenninger, R.; Phan, T.; Gruber, K.; Kratky, C.; Kräutler, B. *Angew. Chem., Int. Ed. Engl.* **1994**, *33*, 889–891.

(14) Scheib, S.; Cava, M. P.; Baldwin, J. W.; Metzger, R. M. *J. Org. Chem.* **1998**, *63*, 1198–1204.

(15) Boyer, B.; Lamaty, G.; Moussamou-Missima, J. M.; Pavia, A. A.; Pucci, B.; Roque, J. P. *Tetrahedron Lett.* **1991**, *32*, 1191–1194.

Scheme 1<sup>a</sup>

<sup>a</sup> (a)  $\text{Na}_2\text{S}_2\text{O}_4$ , DMF, 100 °C, 98%; (b)  $\text{CH}_2\text{CH}(\text{CH}_2)_9\text{OTs}$ ,  $\text{K}_2\text{CO}_3$ , acetone, reflux, 75%; (c)  $\text{CH}_3\text{COSH}$ , AIBN, THF, MeOH, 75 °C, 71% (d) 0.5 M HCl, THF, MeOH, 70 °C, 98%.

differences can be seen, including the thickness, the molecular packing density, the thiolate chemisorption pattern, and the functionality at the monolayer-air/liquid interface. While the aliphatic chains are nearly "isolated" by the bulky penttiptycene groups in the stand-up structure, the folding of aliphatic chains allows side-by-side interchain interactions and, thus, creates one-dimensional stripes. It should be noted that, for a certain tilt angle ( $\alpha$ ) of alkanethiol chain, the dihedral angle ( $\chi$ ) defined by the central benzene ring of the penttiptycene group and the surface plane could be variable, which will be associated with the stripe-to-stripe spacing (vide infra). The following studies were carried out to elucidate the molecular conformations as well as the monolayer assembly structure of  $\alpha,\omega$ -dithiol **1**.

The relative gas phase conformational energies of the extended vs folded conformation of **1** were calculated using the MM2 force field.<sup>19</sup> The results of calculations suggest that the folded conformation should be ca. 6 kcal/mol lower in energy than the extended one, mainly due to the torsional and van der Waals energies. While the torsional energy disfavors the folded conformation by 3 kcal/mol, the approach of the aliphatic chains increases the van der Waals interactions by 9 kcal/mol. The folded conformation (Figure 4) was also used to build the monolayer assembly structure. The width of the folded **1** is ca. 6.5 Å, and an optimum alkanethiol chain distance is 4–5 Å. Accordingly, a side-by-side assembly of the folded **1** will give an intermolecular distance of ca. 10 Å (6.5 Å plus a 3.5 Å of van der Waals spacing) and a spacing of 5 Å between the sulfur heads in the stripes (Figure 3B). The stripe-to-stripe distance will then depend on the orientations of the bulky penttiptycene groups, which can be described by the combination of the tilt angle  $\alpha$  and the dihedral angle  $\chi$ . However,  $\alpha$  and  $\chi$  should not be completely independent. The optimized dihedral angle between the plane containing the two alkanethiol chain and the central benzene ring of the

penttiptycene groups is ca.  $\sim 74^\circ$ . If this angle is retained in the construction of SAMs of the folded **1**, the  $\chi$  values will be either ( $\alpha + 16^\circ$ ) or ( $\alpha - 16^\circ$ ), depending on the tilt to the right or the left of the surface normal. For example, the  $\chi$  value will be either  $14^\circ$  or  $46^\circ$  for a tilt angle of  $30^\circ$ . Within a suitable van der Waals distance between atoms, a stripe-to-stripe spacing of  $\sim 11.5$  Å can be roughly estimated when  $\alpha$  is  $\sim 30^\circ$  and  $\chi$  is  $\sim 14^\circ$ , and other ( $\alpha, \chi$ ) combinations will give larger stripe separations. The corresponding packing density of such an assembly will be  $\sim 115$  Å<sup>2</sup> ( $10 \times 11.5$ ) per molecule, which should be considered as a lower limit. On the basis of the lower calculated conformational energy, denser packing, and shorter chain separation, the folded model (Figure 3B) appears to be superior to an extended structure for **1** on the metal surface. Indeed, atomically resolved STM images support this view.

STM has been a powerful technique in characterizing the structure of organosulfur SAMs.<sup>20</sup> The in situ STM image shown in Figure 5A reveals the arrangement of  $\alpha,\omega$ -dithiol **1** chemisorbed on a well-defined Pt(111) surface (see Experimental Section for details). The ordered domains consisting of protruding stripes form local structures in a scan area of  $50 \times 50$  nm. The domains are mostly 5–7 nm long and 3–5 nm wide. A close-up view of one of these domains, imaged with a 300 mV sample bias voltage and a 3 nA set-point-current, is shown in Figure 5B. The pairwise appearances of the dithiol ends with a separation of 4.5–5 Å in the stripes are in accord with a side-by-side molecular assembly depicted in Figure 3B. On the basis of the predetermined atomically resolved substrate azimuth (figure not shown) and the observed multiple rotational domains (Figure 5A), a unit cell of ( $2\sqrt{7} \times \sqrt{13}$ ) might define the symmetry of this ordered array (Figure 5C). This arrangement gives an averaged spacing of  $\sim 10$  Å between the neighboring stripes. The striped phases have been observed for both short chain alkanethiols ( $\text{C}_4$  and  $\text{C}_6$ )<sup>21</sup>

(19) Chem 3D Plus, Cambridge Scientific Computing, Inc.

(20) Poirier, G. E. *Chem. Rev.* **1997**, *97*, 1117–1127.

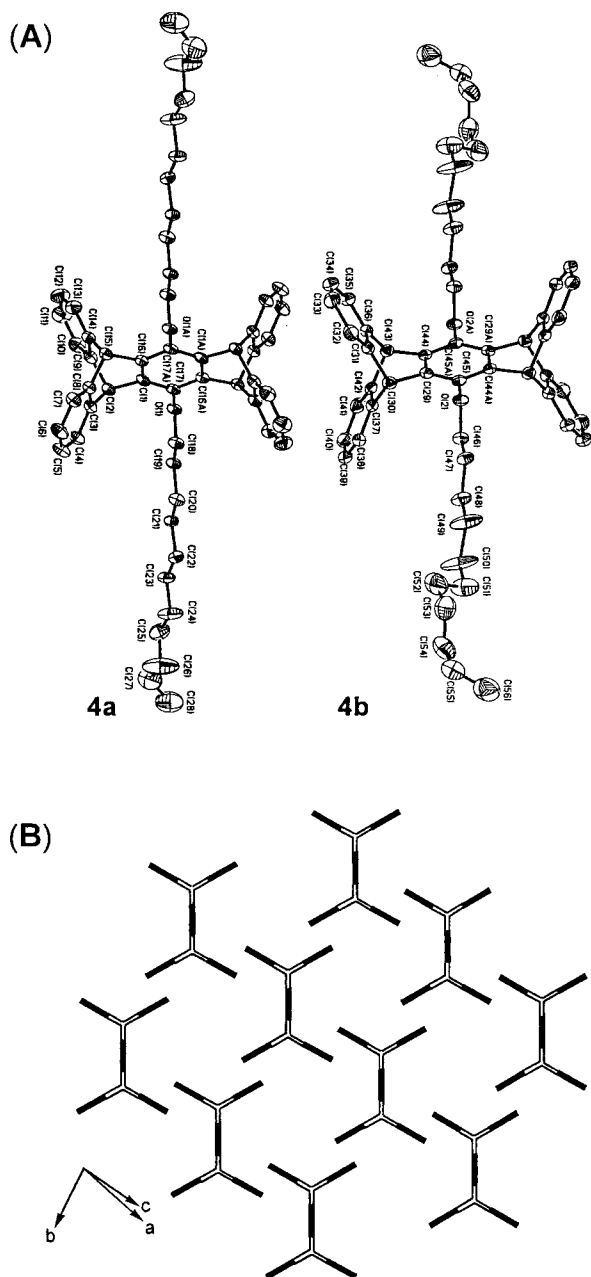


**Figure 2.** (A) The single-crystal X-ray ORTEP (50% probability) structures of two crystallographically independent conformers **4a** and **4b**, and (B) a schematic representation of the arrangement of pentiptycene groups in a two-dimensional layer constructed by **4a** or **4b**.

and  $\alpha,\omega$ -alkanedithiols<sup>6</sup> containing thiophene groups on the gold surface, but their stripe-to-stripe spacings are all larger than 10 Å (e.g., 23–29 Å for butanethiol). Since each unit cell contains one and a half molecule of dithiol **1**, a molecule is estimated to occupy a  $\sim 95$  Å<sup>2</sup> area. The poor solubility of **1** under the experimental conditions might be responsible for its low coverage and subsequently the patchy ordered domains. This situation was not improved by prolonged in situ STM imaging. Other attempts to obtain images with larger ordered domains have been unfortunately unsuccessful.

Surface plasmon resonance (SPR) spectroscopy has been increasingly used in the determination of monolayer

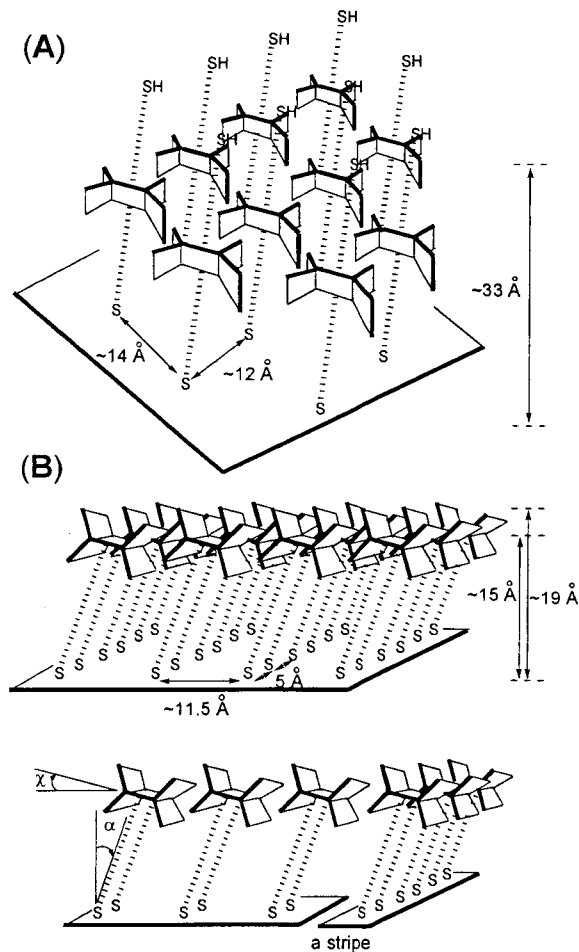


**Figure 3.** Schematic representations of two proposed mono-layer assembly structures of  $\alpha,\omega$ -dithiol **1** on the metal surface: (A) an extended conformation and the corresponding stand-up structure, and (B) a folded conformation and the corresponding looped structure, in which separated figures showing the neighboring molecules in the same stripe and adjacent stripes are included for clarity. See text for the definition of the angles of  $\alpha$  and  $\chi$ .

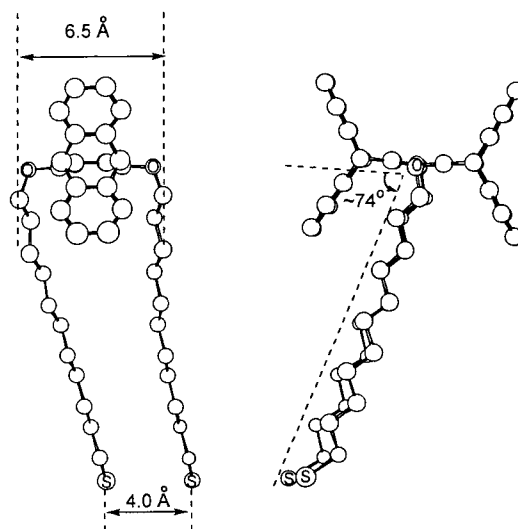


**Figure 4.** Two different views of the MM2 calculated gas-phase folded conformation of  $\alpha,\omega$ -dithiol **1**.

thickness as well as other film properties due to the instrumental simplicity, sensitivity, and stability.<sup>22</sup> Since

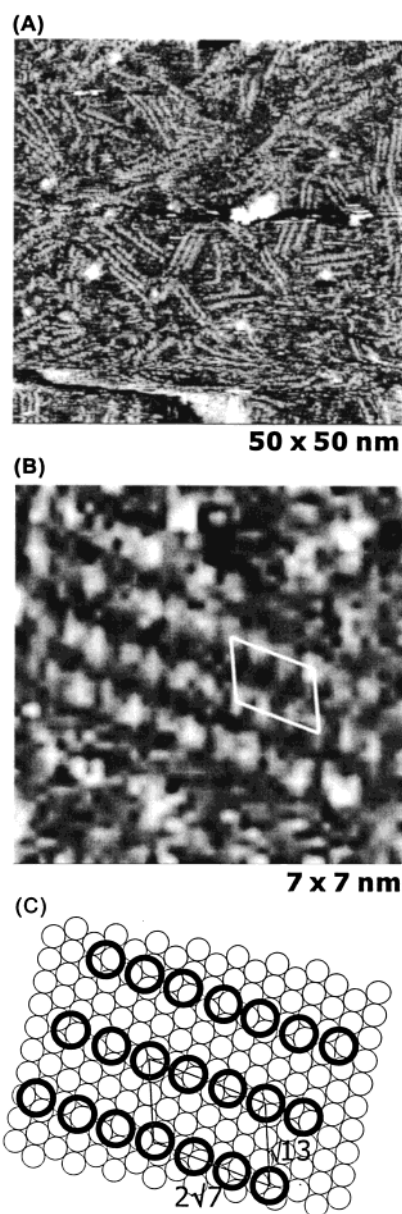


**Figure 5.** (A) A  $50 \times 50$  nm in situ STM image of  $\alpha,\omega$ -dithiol **1** on Pt(111) showing the small ordered domains of striped structure, (B) a close-up view of one of these ordered domains, and (C) the corresponding  $2\sqrt{7} \times \sqrt{13}$  overlayer lattice.

the monolayer thickness of **1** is different for a stand-up vs looped structure, it provides another criterion for the structural characterization. In our ex situ SPR experiments, three independent sample preparations and measurements were carried out at different sample concentrations ( $1 \times 10^{-4}$  to  $5 \times 10^{-5}$  M in THF) and immersion time (20–48 h) to establish the consistency. The typical SPR reflectivity curves for a clean gold surface before and after the chemisorption of **1** along with curve fitting are

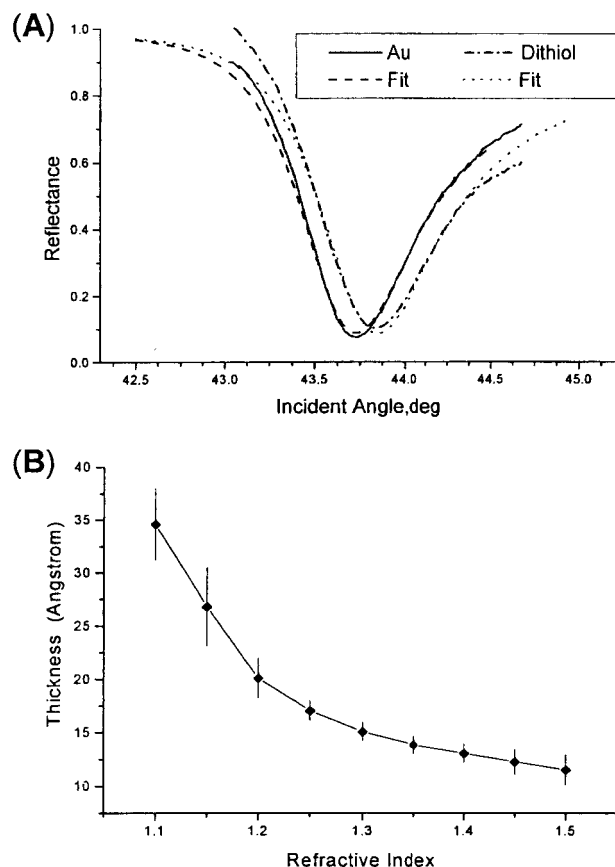


**Figure 6.** (A) The typical SPR reflectivity curves and curves fit for a gold film before and after the chemisorption of  $\alpha,\omega$ -dithiol **1**, and (B) the dependence of the calculated monolayer thickness on the monolayer refractive index. The vertical bars show the deviations in three independent measurements.

shown in Figure 6A. The dependence of the monolayer thickness on the values of monolayer refractive index used for calculation is shown in Figure 6B. The assumption of a refractive index of 1.48 for pure dithiol **1**, a value estimated based on pure benzene ( $n = 1.50$ ) and alkanethiols ( $n = 1.45$ ),<sup>23</sup> will lead to the monolayer thickness in the range of 11–15 Å. However, a lower value than 1.48 appears to be more appropriate in considering the monolayer refraction property, in views of the fact that the structural feature of dithiol **1** will result in a molecular packing less densely than that of benzene or alkanethiols, particularly in the case of a patchy ordered monolayer (Figure 5A). As a consequence, the values of monolayer thickness should be larger than 11–15 Å. On the other hand, to double the monolayer thickness in case of a stand-up monolayer structure ( $\sim 33$  Å), a refractive index of 1.15 or lower should be inserted, a value that is too low to be considered as a reasonable monolayer. The SPR thickness measurements thus suggest that a looped model is more appropriate than a stand-up one in describing the arrangement of **1** on Au(111).

### Concluding Remarks

Unlike the rod-shaped  $\alpha,\omega$ -dithiol systems, which prefer a stand-up conformation on the metal surface

(22) (a) Jordan, C. E.; Frey, B. L.; Kornguth, S.; Corn, R. M. *Langmuir* **1994**, *10*, 3642–3648. (b) Thoden van Velzen, E. U.; Engbersen, J. F. J.; Reinhoudt, D. N. *J. Am. Chem. Soc.* **1994**, *116*, 3597–3598. (c) Huisman, B.-H.; Thoden van Velzen, E. U.; M. van Veggel, F. C. J.; Engbersen, J. F. J.; Reinhoudt, D. N. *Tetrahedron Lett.* **1995**, *36*, 3273–3276. (d) Peterlinz, K. A.; Georgiadis, R. *Langmuir* **1996**, *12*, 4731–4740. (e) Friggeri, A.; M. van Veggel, F. C. J.; Reinhoudt, D. N. *Langmuir* **1998**, *14*, 5457–5463. (f) Jung, L. S.; Campbell, C. T.; Chinowsky, T. M.; Mar, M. N.; Yee, S. S. *Langmuir* **1998**, *14*, 5636–5648.

(23) *23 Handbook of Chemistry and Physics*; Lide, D. R., Ed.; CRC Press: Boca Raton, 1997.

having the second thiol groups located at the monolayer-air/liquid interface.<sup>6–8</sup> the pentiptycene-incorporated  $\alpha,\omega$ -alkanedithiol **1** is able to orient in a looped structure with both the thiol groups bound to the same Pt(111) surface (or Au(111) as well). For parent  $\alpha,\omega$ -alkanedithiols, a stand-up monolayer structure can be formed in a way similar to that of alkanethiols, whereas the formation of a looped structure would require a folding of the molecular backbone, which may lead to torsional strains and less denser packing on the metal surface. In the case of **1**, the bulky pentiptycene groups prevent the aliphatic chains from close contact in a stand-up monolayer structure. In contrast, the folding of the aliphatic chains not only causes a lower conformational energy due to intramolecular chain interactions but also allows molecules to pack in a side-by-side manner having an optimum 5 Å chain-to-chain separation. The pairwise thiolate chemisorption definitely plays an important role in the formation of such a unique looped monolayer structure. Without the second thiolate chemisorption, a monothiol analogue of **1** might not be able to induce any structural ordering on the metal surface. Our data cannot exclude the possibilities of **1** adopting stand-up structures on the border of looped domains. In addition, we cannot distinguish if the pairwise thiolate chemisorption of **1** on the metal surface occurs simultaneously or in a sequence at current stage. It is more likely that the SAM of **1** is not macroscopically ordered, but consists of small domains of the looped structure with stripes arranging in a rotated molecular lattice (Figure 5A). Disregarding of the macroscopic ordering, the looped structure of **1** exposes the nonplanar and  $\pi$ -electron-rich pentiptycene functionalities at the monolayer–air or monolayer–liquid interface, which deserves further investigation. Studies on the supramolecular chemistry of this system by SPR are ongoing, and the results will be reported in its due course.

## Experimental Section

**Scanning Tunneling Microscopy.** The in situ STM experiments were performed with a Nanoscope E machine (Santa Barbara, California). The tips were tungsten wire ( $\times 91\text{\AA}$ , 0.3 mm), electrochemically etched with 30 V DC in 2 M KOH. To minimize the interference of faradic current, the tips were painted with nail polish for insulating. The preparation of Pt(111) electrodes followed a well-known procedure.<sup>24</sup> All the STM experiments were conducted in aqueous solutions containing 0.1 M HClO<sub>4</sub> of electrolyte under potential control, which will result in considerable charging current at the STM tip electrodes. The feedback current (3 nA) had to be set higher than 1 nA in order to diminish the interference of the charging effect with the tunneling process. On the other hand, higher current (>5 nA) enhanced tip-and-sample interactions and eventually degraded the quality of STM results. Prior to dosing Pt(111) with dithiol **1**, the well-defined surface state of Pt(111) was established. The dosing procedure was performed at 0.4 V, and a STM image showing poorly ordered protrusions at terraces was recorded once the toluene solution of **1** was added to the aqueous solution. The constant-current STM images showing small ordered domains were obtained by stepping potential from 0.4 to 0.15 V followed by 5 min of waiting at 0.15 V. This was to be compared to a blank test using toluene solvent under the same experimental conditions, in which only Pt(111) surface could be found. It is believed that our images resulted from electrons tunneling between the

STM tip and the Pt-bound sulfur headgroups.<sup>25</sup> The use of Pt(111) instead of Au(111) was due to the superior reductive capability of the former toward aromatics, leaving behind dithiol **1** attached to the Pt(111) surface.<sup>26</sup>

**Surface Plasmon Resonance.** The SPR spectra were determined using a setup in an ATR (attenuated total reflection) configuration,<sup>27</sup> where p-polarized laser light (He–Ne, 6328 Å) was coupled into a gold film deposited onto a glass microscope slide that is then index-matched to a prism ( $n = 1.515$ ). The gold films employed for our experiments were  $\sim 450$  Å and prepared by an electron beam gun (Temescal SITH270-27M) in a high vacuum chamber with a cryo pump (AISIN GA-16). The reflected light intensity as function of the angle of incidence was detected by a photodiode. The monolayer of dithiol **1** was prepared by immersing Au(111) in the THF solution of **1** (0.1–0.05 mM, 20–48 h), followed by rinsing with THF and drying under an infrared heating lamp for ca. 20 s. The thickness of the gold and monolayer films was obtained by the curve fitting<sup>28</sup> on the corresponding SPR spectra.

**Materials.** All solvents were reagent grade (Merck or Mallinckrodt) unless otherwise noted. THF (HPLC grade) was dried by sodium metal, and acetone was dried with calcium chloride before use. All other compounds were used as received. Pentiptycene quinone<sup>11</sup> **2** and 11-undecenyl tosylate<sup>15</sup> were prepared according to the literature procedures.

**6,13-Dihydroxy-5,7,12,14-tetrahydro-5,14-[1',2']-7,12-[1'',2'']-dibenzopentacene (3).** NaHCO<sub>3</sub> (6.5 g, 0.078 mol) and Na<sub>2</sub>S<sub>2</sub>O<sub>4</sub> (6.5 g, 0.37 mol) were added to a solution of **2** (5 g, 0.011 mol) in DMF (100 mL). The mixture was heated under N<sub>2</sub> at 100 °C overnight, during which time three additional portions of 6.5 g of Na<sub>2</sub>S<sub>2</sub>O<sub>4</sub> were added. The cooled solution was poured into 500 mL of water, and the white precipitate was collected and dried under vacuum to afford **3** in 98% yield (mp > 300 °C, lit.<sup>29</sup> mp 427–430 °C): <sup>1</sup>H NMR (CDCl<sub>3</sub>) 5.48 (s, 2H), 5.68(s, 4H), 6.90 (dd,  $J = 5.4$  and 3.2 Hz, 8H), 7.30 (dd,  $J = 5.4$  and 3.2 Hz, 8H) ppm.

**6,13-Bis(10-undecenyl)-5,7,12,14-tetrahydro-5,14-[1',2']-7,12-[1'',2'']-dibenzopentacene (4).** A mixture of pentiptycene hydroquinone **3** (1.14 g, 2.47 mmol), 11-undecenyl tosylate (1.98 g, 6.16 mmol), and K<sub>2</sub>CO<sub>3</sub> (0.93 g, 6.79 mmol) in 15 mL of dry acetone was refluxed under N<sub>2</sub> for 5 days. The solution was cooled, and then 100 mL of CH<sub>2</sub>Cl<sub>2</sub> was added. The insoluble residue was filtered off, and the filtrate was concentrated under reduced pressure to afford the crude product. Recrystallization in CHCl<sub>3</sub>/MeOH provided the product in needle-type crystals with a 75% yield (mp 177–179 °C): <sup>1</sup>H NMR (CDCl<sub>3</sub>): 1.3–1.7 (m, 24H), 1.9–2.1 (m, 8H), 3.90 (t,  $J = 6.7$  Hz, 4H), 4.9–5.1 (m, 4H), 5.64 (s, 4H), 5.7–5.9 (m, 2H), 6.93 (dd,  $J = 5.3$  and 3.1 Hz, 8H), 7.29 (dd,  $J = 5.3$  and 3.1 Hz, 8H) ppm; <sup>13</sup>C NMR (CDCl<sub>3</sub>): 26.43, 28.98, 29.18, 29.57, 29.65, 29.70, 30.56, 33.84, 48.40, 76.13, 114.19, 123.51, 125.08, 136.22, 139.20, 145.40, 146.09 ppm; IR (KBr): 1025, 1258, 1460, 1692 cm<sup>-1</sup>. Anal. Calcd for C<sub>56</sub>H<sub>62</sub>O<sub>2</sub>: C, 87.68, H, 8.15. Found: C, 87.69, H, 8.23.

**6,13-Bis(11-acetylthioundecanoxy)-5,7,12,14-tetrahydro-5,14-[1',2']-7,12-[1'',2'']-dibenzopentacene (5).** To a solution of **4** (1.1 g, 1.30 mmol) and AIBN (1 g, 6.09 mmol) in 15 mL of THF under argon was added 1.5 mL of thioacetic acid (2.1 mmol). The mixture was then heated at 75 °C overnight. The solvent was removed, and methanol was then added to the residue. The resulting white solid was collected by filtration. Column chromatography using CH<sub>2</sub>Cl<sub>2</sub> as eluent afforded dithioester **5** (0.9 g, 71%) (mp 175–177 °C): <sup>1</sup>H NMR (CDCl<sub>3</sub>): 1.1–1.7 (m, 32H), 1.99 (q,  $J = 6.8$  Hz, 4H), 2.30 (s, 6H), 2.87 (t,  $J = 6.9$  Hz, 4H), 3.88 (t,  $J = 6.6$  Hz, 4H), 5.62 (s, 4H), 6.85 (dd,  $J = 5.2$  and 3.2 Hz, 8H), 7.23 (dd,  $J = 5.2$  and

(25) Widrig, C. A.; Alvas, C. A.; Porter, M. D. *J. Am. Chem. Soc.* **1991**, *113*, 2805–2810.

(26) Schmiemann, U.; Jusys, Z.; Baltruschat, H. *Electrochim. Acta* **1994**, *39*, 561–576.

(27) Salamon, Z.; Macleod, H. A.; Tollin, G. *Biochim. Biophys. Acta* **1997**, *1331*, 131–152.

(28) Lee, C.-C.; Jen, Y.-J. *Appl. Optics* **1999**, *38*, 6029–6033.

(29) Hart, H.; Shamouilian, S.; Takehira, Y. *J. Org. Chem.* **1981**, *46*, 4427–4432.

(24) Clavilier, J.; Rodes, A.; Achi, K. E.; Zamakhchari, M. *J. Chim. Phys.* **1991**, *88*, 1291–1337.

3.2 Hz, 8H) ppm;  $^{13}\text{C}$  NMR ( $\text{CDCl}_3$ ): 26.44, 28.85, 29.17 (2C), 29.53 (2C), 29.65, 29.71, 30.57, 30.62, 48.41, 76.13, 123.50, 125.08, 136.22, 145.28, 146.09, 196.02 ppm; IR (KBr): 1111, 1255, 1461, 1680  $\text{cm}^{-1}$ . Anal. Calcd for  $\text{C}_{60}\text{H}_{70}\text{O}_4\text{S}_2$ : C, 78.39, H, 7.67, S, 6.98. Found: C, 78.35, H, 7.63, S, 7.02.

**6,13-Bis(11-mercaptoundecanoxy)-5,7,12,14-tetrahydro-5,14[1',2':7,12-[1'',2'']-dibenzopentacene (1).** The deprotection of the acetyl group was carried out by dissolving dithioester **5** (0.6 g, 0.6 mmol) in a mixture of 50 mL of THF/MeOH (1:1) containing 0.5 M of HCl and stirring at 70 °C for 48 h. The solvent was removed and methanol was then added to the residue. The resulting white solid was collected by filtration to yield dithiol **1** (0.56 g, 98%). Further purification was performed by recrystallization in  $\text{CHCl}_3/\text{MeOH}$ . (mp 204.5–205 °C).  $^1\text{H}$  NMR ( $\text{CDCl}_3$ ): 1.2–1.7 (m, 32H), 2.03 (q,  $J = 7.0$  Hz, 4H), 2.51 (q,  $J = 7.0$  Hz, 4H), 3.89 (t,  $J = 6.7$  Hz, 4H), 5.63 (s, 4H), 6.93 (dd,  $J = 5.3$  and 3.2 Hz, 8H), 7.29 (dd,  $J = 5.3$  and 3.2 Hz, 8H) ppm;  $^{13}\text{C}$  NMR ( $\text{CDCl}_3$ ): 24.65, 26.43, 28.40, 29.12, 29.56, 29.65, 29.72 (2C), 30.55, 34.05, 48.41,

76.11, 123.50, 125.08, 136.21, 145.40, 146.09 ppm; IR (KBr): 1035, 1257, 1460  $\text{cm}^{-1}$ ; Anal. Calcd for  $\text{C}_{56}\text{H}_{66}\text{O}_2\text{S}_2$ : C, 80.53, H, 7.96, S, 7.68. Found: C, 80.52, H, 7.90, S, 7.63.

**Acknowledgment.** Financial support for this research was provided by the National Science Council (NSC 88-2113-M-008-011 and NSC 89-2113-M-008-002). J.S.Y. is also grateful for a start-up fund from the National Central University. We thank Professors K.-W. Lii (NCU) and S.-M. Peng (NTU) and Mr. G.-H. Lee (NTU) for resolving the crystal structure of **4**, and a reviewer for helpful suggestions.

**Supporting Information Available:** Tables and Figures of detailed crystallographic data and packing of compound **4**. This material is available free of charge via the Internet at <http://pubs.acs.org>.

JO991339A